https://doi.org/10.5194/acp-2020-823
Preprint. Discussion started: 14 January 2021

Atmospheric Chemistry and Physics Discussions

Atmospheric transmission patterns which promote persistent winter haze over Beijing

Muyuan Li[1,2], Yao Yao[1,2], Ian Simmonds[3], Dehai Luo[1,2], Linhao Zhong[1,2], Lin Pei[4]

[1]Key Laboratory of Regional Climate-Environment for Temperate East Asia, Institute of Atmospheric Physics, Chinese Academy of Sciences, Beijing, 100029, China

[2]University of Chinese Academy of Sciences, Beijing, 100049, China

[3]School of Earth Sciences, University of Melbourne, Parkville, Victoria, 3010, Australia

[4]Institute of Urban Meteorology, China Meteorological Administration, Beijing, 100089, China

Correspondence to: Yao Yao (yaoyao@tea.ac.cn)

Abstract. The persistent winter haze episodes that occurred in Beijing over the period 1980 to 2016 are examined based on both reanalysis and station data. On both interannual and intra-seasonal timescales, winter haze weather in Beijing is found to be associated with a significant atmospheric teleconnection pattern from the North Atlantic to Eurasia (Beijing). A positive North Atlantic Oscillation (NAO+) phase and a positive East Atlantic/West Russia (EA/WR+) phase can be observed as part of this teleconnection pattern (or an arched wave train). This study focuses mainly on the role of the NAO+ pattern, because the NAO index shows a closer relationship with winter haze frequency, especially after 1999, and the NAO+ pattern leads to the formation of persistent haze events over a longer period of time. Composite analyses show that a robust and consistent daily evolution of the wave train originates from an NAO+ pattern over the North Atlantic 8–10 days prior to the persistent haze events. The wave train continues propagating energy downstream, which leads to the formation and maintenance of a high-pressure center over northeast China, thus creating favorable meteorological conditions for the persistent haze events in Beijing. Thus, the NAO+ pattern is also an essential preceding background for the formation of the wave train, which can be treated as a potential predictor for persistent hazy weather. Corresponding to the NAO+ pattern, a tripolar sea surface

https://doi.org/10.5194/acp-2020-823
Preprint. Discussion started: 14 January 2021


Atmospheric Chemistry and Physics Discussions

temperature mode and intensified zonal wind over the North Atlantic also serve as prior signals for the persistent haze events. In addition, the propagation of the wave train is also associated with preceding significant positive sea ice concentration anomalies in the Barents–Kara Sea. Moreover, comparative analysis demonstrates that NAO+ winters are more advantageous to the formation and maintenance of winter haze weather in Beijing rather than NAO− winters.

1 Introduction

Beijing, the capital city of China, is situated in the northeast of the country. It covers 16,410 km^2 and has a permanent population of 21.542 million. In 2019 Beijing's gross domestic product reached 3,537 billion yuan, an increase of 6.1 % over the previous year (http://www.stats.gov.cn). Along with economic development, Beijing has had more frequent hazy weather, especially persistent haze in winter, over the last 60 years (Wang et al., 2014; Su et al., 2015; Li et al., 2018a; Pei and Yan, 2018; Pei et al., 2018; Shi et al., 2019). Haze pollution is associated with a high $PM_{2.5}$ concentration and low visibility, and is harmful to human health (e.g., cardiovascular and respiratory diseases and lung cancer) and puts pressure on public transportation and economic activities (Wang et al., 2013).

The serious impacts of haze pollution in Beijing have been the topic of numerous studies. High emissions of haze pollutants (e.g., black carbon and organic matter) contribute greatly to the formation of hazy weather in Beijing (Li and Han, 2016; Wu et al., 2016; Li et al., 2017). In addition, the atmospheric and meteorological conditions as well as external and remote influences, such as Arctic sea ice concentration (SIC), snow cover across Siberia, and sea surface temperature (SST), should also be taken into consideration (An et al., 2019; Wang et al., 2020). Atmospheric circulations that are favorable for hazy weather in Beijing include a weak East Asian winter monsoon (EAWM), a shallow

https://doi.org/10.5194/acp-2020-823
Preprint. Discussion started: 14 January 2021


Atmospheric Chemistry and Physics Discussions

East Asian trough and a northward shift of the East Asian jet (Chen and Wang, 2015; Zou et al., 2017; Pei et al., 2018; Wang et al., 2020). These circulations tend to reduce the intrusion of cold air to Beijing, and hence result in poor ventilation conditions in winter (Zou et al., 2017; Pei et al., 2018). Furthermore, teleconnection patterns and wave trains also have potential impacts on haze over Beijing (Yin and Wang, 2017; Yin et al., 2017; Chen et al., 2019; Zhang et al., 2019; Chen et al., 2020a, 2020b; Lu et al., 2020). Yin et al. (2017) analyzed the roles of the positive phases of the East Atlantic/West Russia (EA/WR+) pattern, the western Pacific pattern, and the Eurasia pattern in the increased number of hazy days over the North China Plain. They found that these climatic anomalies could lead to meteorological conditions that are conducive to the formation of haze pollution through modulating the anticyclonic anomalies over north China (Yin and Wang, 2017; Yin et al., 2017). The positive phase of the Arctic Oscillation (AO+) pattern can also increase the number of hazy days in Beijing (Lu et al. 2020). Years with high AO indices are accompanied by a weakened East Asian trough and a weakened Siberian high, which suppress the vertical diffusion of haze pollutants (Lu et al. 2020). Chen et al. (2019) stressed the role of the positive phase of the North Atlantic Oscillation (NAO+), which is related to AO+, in inducing an anticyclone over northeast China, which favors haze pollution in north China in spring. Chen et al (2020b) also looked at autumn haze, and found the relative importance of the external drivers seems to differ across the individual months of September, October and November. Additionally, the winter haze weather in Beijing is directly affected by the local meteorological conditions. Many studies have suggested that static and relatively warm air, weakened northerly or even southerly winds, decreased relative humidity, temperature inversions and downward air motion in the planetary boundary layer can suppress the dispersal and advection of haze pollutants (Wang et al., 2014; Zhang et al., 2014; Zhang et al., 2016; Wu et al., 2017; Wang et al. 2019; Zhong et al., 2019).

https://doi.org/10.5194/acp-2020-823
Preprint. Discussion started: 14 January 2021


Atmospheric Chemistry and Physics Discussions

In line with the suggestion above a reduction in Arctic sea ice in autumn could increase subsequent winter haze days through weakening wave activity over eastern China (Wang and Zhang, 2015; Zou et al., 2017). Zou et al. (2017) also revealed that increased Eurasian snowfall in earlier winter leads to regional circulations unfavorable to the ventilation of pollutants. Furthermore, autumn Beaufort Sea ice can be closely connected with the number of early-winter haze days in north China (Yin et al., 2019a; Li and Yin, 2020), while an increase in early-winter Chukchi Sea ice can intensify February haze pollution in north China (Yin et al., 2019b). The changes in sea ice in both the Beaufort Sea and the Chukchi Sea are linked with hazy weather in north China via modulated large-scale atmospheric circulations (e.g., the East Asian trough and teleconnections). SSTs in both the Atlantic and Pacific have potential impacts on the occurrence of hazy weather (Xiao et al., 2015; Pei et al., 2018; Wang et al., 2019). Winter haze days in China are also associated with SST anomalies over the North Atlantic on decadal and interannual timescales via the Atlantic multidecadal oscillation, and are also related to SSTs over the South Atlantic on interannual timescales by anomalous southerly airflow (Xiao et al., 2015). Pei et al. (2018) found that positive SST anomalies over the northwest Pacific are conducive to more winter haze days in Beijing by weakening the EAWM system. Wang et al. (2019) also suggested that the interannual variability in autumn haze days in the Beijing–Tianjin–Hebei region is associated with a wave train induced by SSTs in the North Atlantic subtropics and a local meridional cell induced by SSTs in the western North Pacific.

Persistent haze events correspond to continuous pollution for several days, which not only has a broad impact on human life (through traffic jams, for example), but also threatens human health to a deeper degree. In this study, we gain a better understanding of the physical processes and mechanisms of the persistent haze over Beijing. Local meteorological conditions are directly associated with hazy

https://doi.org/10.5194/acp-2020-823
Preprint. Discussion started: 14 January 2021


Atmospheric Chemistry and Physics Discussions

91 weather and usually show diurnal variations (Zhang et al., 2014; Li et al., 2018b; Li et al., 2019), while
92 external forces, which vary slowly, play key roles in explaining the interannual/interdecadal
93 variabilities in hazy weather (Wang et al., 2020). On intra-seasonal timescales, large-scale atmospheric
94 circulations (e.g., teleconnections and wave trains) can bridge the timescales of local meteorological
95 conditions and external forces. Atmospheric circulations can be modulated by external forces and
96 meanwhile can influence local meteorological conditions. In previous studies, the atmospheric patterns
97 associated with hazy weather were mainly obtained from linear correlation or composite analysis based
98 on interannual or longer timescales (Yin and Wang, 2017; Yin et al., 2017; Chen et al., 2019; Lu et al.,
99 2020). However, the evolution of these atmospheric circulations and their roles in the formation of
100 hazy weather (especially persistent haze events) from daily to intra-seasonal timescales are not clear.
101 Thus, a more in-depth analysis of daily changes is needed to build a more solid relationship between
102 haze and atmospheric circulation, and to provide us with more hints for haze forecasting if certain
103 circulation patterns could be verified several days before persistent haze events. This will help to
104 improve predictive skills for persistent haze over Beijing. In this study, we focus mainly on persistent
105 winter haze over Beijing and the corresponding large-scale atmospheric circulations from the
106 perspectives of interannual and daily timescales. In particular, we are interested in the role of the
107 NAO+ pattern in the early stage of the formation of haze events. We also investigate the conditions of
108 SSTs and Arctic Sea ice that have been proposed as drivers of large-scale atmospheric circulations.
109 Furthermore, persistent haze events related to NAO+ and NAO− patterns are examined and compared.

110 **2 Data and methods**

111 **2.1 Data**

112 The observed relative humidity and visibility at 20 stations in Beijing at four local times (02:00,

https://doi.org/10.5194/acp-2020-823
Preprint. Discussion started: 14 January 2021


Atmospheric Chemistry and Physics Discussions

113 08:00, 14:00 and 20:00) each day from 1980 to 2016 during the winter (December, January and
114 February (DJF)) are obtained from quality-controlled station observations at the National Mereological
115 Information Center of China. Daily means of these variables are then calculated. Reanalysis data are
116 taken from the European Centre for Medium-Range Weather Forecasts (ECMWF) ERA-Interim on a
117 1 ° × 1 ° grid (Dee et al., 2011). The variables include daily geopotential height at 500 hPa (Z500),
118 horizontal winds (at 500, 850 and 925 hPa), temperature (at 500, 700, 850 and 925 hPa), relative
119 humidity (at 500, 700, 850 and 925 hPa), SST, sea level pressure (SLP) and boundary layer height
120 (BLH). We also used monthly SST and SIC data from the Hadley Centre Global Sea Ice and Sea
121 Surface Temperature (HadISST) dataset (Rayner et al., 2003).

122 We use the normalized NAO index and EA/WR index from the National Oceanic and
123 Atmospheric Administration/Climate Prediction Center (NOAA/CPC). Our investigation also employs
124 a second NAO index (referred to hereafter as a modified LW03 NAO index), which is a modification
125 of that proposed by Li and Wang (2003). Those authors defined an NAO index as the difference in the
126 normalized SLP, zonally averaged from 80° W to 30° E, between 35° N and 65° N. They commented
127 that this measure 'provides a much more faithful and optimal representation of the spatial–temporal
128 variability associated with the NAO'. We have made this modification for our study because this
129 longitudinal range includes both the North Atlantic and part of the European continent. Atmospheric
130 circulations in our investigation involve both a blocking anticyclone over Europe (EB) and an NAO
131 pattern. When the anticyclone over Europe and the NAO pattern occur concurrently, the NAO index
132 of Li and Wang (2003) may have difficulties in interpreting the real NAO pattern, since the surface
133 pressure centered in the north of the NAO pattern is easily distorted by the large geopotential height
134 anomalies over Europe. To avoid this complexity, we have slightly modified the Li and Wang (2003)

https://doi.org/10.5194/acp-2020-823
Preprint. Discussion started: 14 January 2021


Atmospheric Chemistry and Physics Discussions

definition by conducting our sector averaging over 80° W–10° W, instead of the original 80° W–30° E. Such a modification is supported by detailed NAO studies (Yao and Luo 2014; Luo et al. 2014; Yao et al. 2016), which reveal the disadvantage of the prevailing NAO indices in the identification of the spatial structures of the NAO pattern. They also suggested that the zonal position and inclination of the NAO dipole could change the occurrence of extreme weather events.

2.2 Definition of persistent haze events

Haze is generally defined in terms of relative humidity and visibility (World Meteorological Organization, China Meteorological Administration, UK Met Office). In the "Specifications for surface meteorological observations" compiled by the China Meteorological Administration (2004), haze is defined as a weather phenomenon with a large amount of extremely fine dust particles evenly floating in the air, which reduces the horizontal visibility to less than 10 km. Since visibility can also be reduced by fog, a relative humidity threshold is applied to distinguish hazy weather from fog. Many previous studies (Wu, 2006, 2008; Yang et al., 2016; Pei et al., 2018; He et al., 2018) proposed that fogs are associated with a relative humidity greater than 90%. Therefore, we use a daily mean relative humidity of less than 90% and a visibility of less than 10 km as criteria to define winter haze days in this study (Pei et al., 2018; Chang et al., 2020). Persistent haze events are defined as periods for which haze occurs for at least 5 consecutive days.

2.3 Atmospheric thermal stability index

The atmospheric thermal stability index (A_I) is defined according to Zhang et al. (2007), as:

$$A_I = (T_{850} - T_{500}) - [(T_{850} - T_{d850}) + (T_{700} - T_{d700}) + (T_{500} - T_{d500})]$$

where T and T_d represent the temperature and dewpoint, respectively, and the subscripts denote the pressure level.

https://doi.org/10.5194/acp-2020-823
Preprint. Discussion started: 14 January 2021


Atmospheric Chemistry and Physics Discussions

3 Associated large-scale atmospheric circulations

3.1 Interannual variability

To present the context of the relationship between Beijing winter haze weather and atmospheric circulation, in Fig. 1a we show the time series of the number of winter haze days (blue line) and detrended winter haze days (red line) from 1980 to 2016. The linear trend (+1.93 days/decade) of the number of winter haze days in Beijing is not significantly different from zero, which is consistent with previous studies (Chen and Wang, 2015; Pei et al., 2018, 2020), and its interannual variability is quite large. Many factors could affect the variation in number of winter haze days, including changes in emissions, changes in emission reduction measures and climate variables (e.g., meteorological conditions, atmospheric circulation and SSTs) (Dang and Liao, 2019; Wang et al., 2020; Pei et al. 2020). Pei et al. (2020) pointed out that anthropogenic emissions showed an increasing trend before 2012 and a decreasing trend after 2012, which can be attributed to a Clean Air Action Plan introduced in 2013, and the inconsistent trends could explain the absence of a significant trend in the number of hazy days. Thus, we undertake our investigation with detrended data to explore the influences which are associated with the interannual variation in number of hazy days. For the sake of reliability, long-term trends are removed for winter haze days and other variables in the following analyses.

We focus first on the role of atmospheric circulation in hazy weather from interannual timescales. The detrended winter haze days are significantly correlated with circulation patterns in the Z500 anomaly field (Fig. 1b). It is shown that a wave train with a wavenumber-3 structure dominates the mid-high latitudes. Three cyclones are situated over the Greenland region, the Ural region and the Sea of Okhotsk with positive geopotential height anomalies in between (Fig. 1b). Atmospheric teleconnections, namely the NAO+ pattern and the EA/WR+ pattern have been suggested to be

https://doi.org/10.5194/acp-2020-823
Preprint. Discussion started: 14 January 2021


Atmospheric Chemistry and Physics Discussions

connected with winter haze days in Beijing (Yin and Wang, 2017; Yin et al., 2017; Chen et al., 2019). Barnston and Livezey (1987) show the NAO+ pattern to be made up of negative geopotential height anomalies in the high latitudes of the North Atlantic (Greenland) and positive anomalies over the central North Atlantic, extending into the eastern United States and western Europe. The EA/WR+ pattern is associated with positive geopotential height anomalies over Europe and northern China, and negative anomalies located over the central North Atlantic and the north of the Caspian Sea. Following Barnston and Livezey (1987), we can say that Fig. 1b demonstrates an NAO+ pattern over the North Atlantic, although this pattern is situated further to the west and co-occurs with a blocking anticyclone over Europe. In addition, although a quadrupole mode from the North Atlantic to northern China shares some similarities with an EA/WR+ pattern, there are also some differences. On the one hand, two negative geopotential height anomalies are located over the northern North Atlantic and the northern Ural region, which are further north than the two cyclones of the EA/WR+ pattern. On the other hand, the EA/WR+ pattern shows a zonal wave train structure; and only when the cyclone (north center of the NAO+ pattern) over the North Atlantic is excluded, can a tripolar mode from Europe to northern China constitute a zonal wave train structure.

To further understand the relationships between winter haze days in Beijing and teleconnection patterns of NAO and EA/WR, we present the annual variations in winter haze days, the NAO index and EA/WR index from NOAA/CPC, and the modified LW03 NAO index in Fig. 2. Their correlation coefficients are calculated over the time periods 1980–2016, 1980–1999 and 2000–2016. Correlation coefficients between winter haze days and the NOAA/CPC NAO index are 0.27, 0.16 and 0.33, respectively, and only the correlation for the entire 1980–2016 period is significant at the 90% confidence level (Fig. 2a). Considering that the NAO+ pattern assumes a more westerly position

https://doi.org/10.5194/acp-2020-823
Preprint. Discussion started: 14 January 2021


Atmospheric Chemistry and Physics Discussions

because of the presence of the EB in Fig. 1b, this NAO index cannot fully reflect the real relationship between the north–south dipole mode over the North Atlantic and winter haze days in Beijing. For the reasons discussed earlier, our modified LW03 NAO index presents a clearer metric of the NAO for our study. Correlation coefficients between winter haze days in Beijing and the modified LW03 NAO index are considerably larger for the 1980–2016 and 2000–2016 periods, being 0.42 ($p < 0.01$) and 0.61 ($p < 0.01$), respectively, while the correlation coefficient (0.08) is smaller (and nonsignificant) during the period 1980–1999 (Fig. 2b). As for the correlation with the EA/WR index, it is slightly smaller than that with the modified LW03 NAO index for the entire period (0.36, $p < 0.05$), while it is considerably higher (0.57, $p < 0.01$) when only the first 20 years of the record are considered. Overall, we see that the NAO+ pattern is more closely related to winter haze days in Beijing. However, it should be noted that the EA/WR+ pattern has a closer relationship with hazy weather in Beijing before 2000, while the NAO+ pattern is dominant after that date. It is also worth noting that the extreme numbers of winters haze days more closely correspond with the magnitude of the NAO index. Figure 2 shows that the extremely low numbers of hazy days in the winters of 1995, 2003 and 2010 occur simultaneously with small NAO values of −1.11 standard deviation (std dev), −1.11 std dev and −1.61 std dev, respectively, while the winter of 2013 with an extremely high number of hazy days has a large NAO value of 2.42 std dev. However, such correspondences could not be found in the values of the EA/WR index. Thus, we propose that the modified LW03 NAO index is better correlated with winter haze days in Beijing, especially in recent decades (2000–2016), and better explains the extreme values of winter haze days in Beijing.

3.2 Large-scale and local daily atmospheric structure before and after persistent haze events

To cast further light on the above results, we have identified all the persistent haze events over

https://doi.org/10.5194/acp-2020-823
Preprint. Discussion started: 14 January 2021


Atmospheric Chemistry and Physics Discussions

the period 1980–2016, and explored the daily progression of the circulation structures which lead up to (out to 10 days) and follow (out to 8 days) the 65 identified persistent haze episodes. To accomplish this, we formed composites (across the 65 episodes) of daily Z500 anomalies and the horizontal components of wave activity flux (Takaya and Nakamura, 2001). The sequence of the composites is shown in Fig. 3, where Day 0 denotes the day with the minimum visibility within a persistent haze event. From Day −10 to Day −8, an NAO+ pattern can be identified over the North Atlantic, and wave activity flux propagates downstream from the north pole of the NAO+ pattern to a weak anticyclone over Europe. Compared with the NAO pattern in Li and Wang's work (2003), the north–south dipole mode of the NAO pattern here is situated more to the west and is accompanied by an anticyclone over Europe. This is why we use a modified NAO index in this study, which was introduced in Sect. 2. From Day −6 to Day −4, the weak anticyclone over Europe gets stronger and a cyclone develops over western Russia following the propagation of wave activity. Simultaneously, the NAO+ pattern weakens and shows a northeast–southwest inclination. From Day −3 to Day −2, an EA/WR+ pattern is becoming obvious at the mid to high latitudes. At this time, a zonal wave train that propagates from a cyclone over the North Atlantic, through an anticyclone over Europe and a cyclone over the west of Lake Baikal, to East Asia leads to the formation of an anticyclone over northeastern China. On Day −1, an anticyclone forms over the Gulf Stream region, which continues to provide wave activity to the development of downstream circulation. This anticyclone sustains the wave train propagating to northeastern China. As a result, the anticyclone over northeastern China persists for a total of 7 days from Day −3 to Day 3 and then moves eastward to the North Pacific. The wave train structure dissipates from Day 4, and the anomalous atmospheric circulation around Beijing becomes weaker.

From the daily evolution of atmospheric circulation, we find that certain teleconnection patterns

https://doi.org/10.5194/acp-2020-823
Preprint. Discussion started: 14 January 2021


Atmospheric Chemistry and Physics Discussions

(NAO+ and EA/WR+) and wave trains lead to persistent haze events in Beijing, since the formation of teleconnection patterns is closely related to zonal winds, and zonal winds act as waveguides for the propagation of wave trains (Ambrizzi et al., 1995; Fang et al., 2001; Athanasiadis et al., 2010; Wang and Zhang 2015; Martinez-Asensio et al., 2016; Wirth et al., 2018). Zonal wind anomalies at 300 hPa are composited between Day −10 and Day 5 for the 65 persistent haze events to explain the evolution of large-scale circulations and to ascertain whether potential predictors exist (Fig. 4a). Corresponding to the propagation of an NAO+ pattern and an EA/WR+ pattern during the formation of persistent haze events in Beijing, significantly intensified or weakened anomalous zonal wind centers could be clearly identified from the North Atlantic to East Asia. The negative–positive–negative zonal wind tripolar mode over the North Atlantic reflects the NAO+ pattern, while the arched structure of the anomalous zonal wind from Greenland, passing through high latitudes to northern China, manifests in the EA/WR+ pattern. To track the daily variations in anomalous zonal winds, significantly increased zonal wind anomalies over the central North Atlantic, the Scandinavian Peninsula and the north of China are taken as three indicators (Fig. 4b). The amplitude of the anomalous zonal wind over the central North Atlantic peaks at Day −8, which corresponds to the prevalence of the NAO+ pattern from Day −8 to Day −10 in Fig. 3. Although the zonal wind in this region weakens after Day −8, it retains significantly high values until Day 4. Simultaneously with the significantly increased zonal wind over the central North Atlantic, the difference in the zonal wind over the south of the Scandinavian Peninsula and the zonal wind over north China also show significant positive anomalies starting from Day −11 and Day −5, respectively. The difference in the zonal wind over the south of the Scandinavian Peninsula reaches its highest point on Day −2 when the EA/WR+ pattern can be clearly identified in Fig. 3, while the anomalous zonal wind over the north of China reaches a peak on Day −1. From the analyses above,

https://doi.org/10.5194/acp-2020-823
Preprint. Discussion started: 14 January 2021


Atmospheric Chemistry and Physics Discussions

we can see that the three indicators of anomalous zonal winds could well reflect the sequential occurrence of teleconnection patterns related to persistent haze events. These indicators also express the downstream propagation of a wave train from the North Atlantic to northern China. Since the intensified zonal winds over the central North Atlantic, the Scandinavian Peninsula and the north of China are prior to the persistent haze events, they have potential value as predictors for persistent haze events.

From the Day 0 panel of Fig. 3 we note that Beijing is under the influence of an anticyclone, whose center is a short distance to the northeast of the city. This anticyclone could influence the accumulation of haze pollutants in Beijing by modulating the meteorological conditions (Zhong et al., 2019). We now turn our attention to the spatial–temporal variations in the local meteorological conditions related to the anticyclonic circulation (Fig. 5). Figure 5a depicts the spatial distribution of composite anomalous 850 hPa horizontal wind velocity and SLP for the 65 persistent haze events. Beijing is located at the border of anomalous high-pressure areas over mainland China and anomalous low-pressure areas situated over the northwestern Pacific. The weakened pressure gradients between mainland China and the coastal regions indicate a weakened EAWM (Pei et al. 2018). Beijing is controlled by anomalous southerly winds and the wind speeds are significantly less than normal. Together with the vertical downdraft of the anticyclone at 500 hPa, these meteorological conditions militate against the ventilation of pollutants. In addition, daily variations in composite meridional wind component (V), wind velocity, relative humidity, temperature at 925 hPa, BLH and A_I in Beijing are consistent with the poor dispersal of pollutants (Fig. 5b). The BLH decreases rapidly after Day −5, reaches a minimum at Day 0 and then rapidly increases, whereas the temperature shows the opposite variations. The relative humidity and A_I reach their largest values on Day 1. The smaller BLH and

https://doi.org/10.5194/acp-2020-823
Preprint. Discussion started: 14 January 2021


Atmospheric Chemistry and Physics Discussions

289 A_I correspond to stable weather conditions, which also inhibit the dispersal of pollutants. Furthermore,
290 the increased temperature and relative humidity are conducive to the hydroscopic growth of pollutants,
291 which could further aggravate the hazy weather. Though these local meteorological elements are most
292 directly related to persistent haze events in Beijing, they do not show prominent prior changes.

293 **4 External influence of sea surface temperature and sea ice concentration**

294 As noted earlier, previous studies showed that atmospheric circulations are affected by external
295 influences, such as SST and Arctic SIC (Wang and Zhang, 2015; Yin et al., 2017; Chen et al., 2019).
296 Since many of these external forces vary slowly and have significant memory, they may potentially
297 present precursors to persistent haze events. In this section, we relate SST in the North Atlantic and
298 SIC in the Greenland Sea and Barents–Kara Sea with persistent haze events in Beijing via atmospheric
299 circulations.

300 Below we refer to the number of persistent haze days in a winter as the sum of hazy days
301 belonging to persistent haze events of the winter. This measure reflects the number of persistent haze
302 events as well as their duration. The composite distributions of SST anomalies and SIC anomalies of
303 11 winters (1988, 1996, 1998, 2005, 2007, 2008, 2011–15) with more than 15 persistent haze days and
304 11 winters (1980, 1982–84, 1986, 1987, 1994, 1995, 1999, 2003, 2010) with no more than 5 persistent
305 haze days, and their differences are shown in Fig. 6.

306 As shown in Fig. 6a, the SST anomalies associated with the most persistent haze days show a
307 north–south tripolar mode in the North Atlantic, with positive anomalies in the Gulf Stream region and
308 negative anomalies at the southwest of the Canary Islands and regions around Greenland, which is
309 consistent with the NAO+ pattern. Simmonds and Govekar (2014) noted that warm SST in the Gulf
310 Stream region gives rise to a teleconnection pattern with a node in the Barents Sea and another over

https://doi.org/10.5194/acp-2020-823
Preprint. Discussion started: 14 January 2021


Atmospheric Chemistry and Physics Discussions

311 Eurasia. Significant SST anomalies can also be seen in the northwestern Pacific, with the negative SST
312 anomalies from Yellow Sea to the Sea of Japan and positive SST anomalies to the east of the
313 Philippines. These SST anomalies are difficult to explain the atmospheric anticyclone from mainland
314 China to the northwestern Pacific, which is directly related with persistent haze events in Beijing. For
315 SST anomalies of winters with fewer persistent haze days, a north–south tripolar mode in the North
316 Atlantic could be found opposite to that in Fig. 6a, though the anomalies are not significant (Fig. 6b).
317 In addition, significant positive SST anomalies are located at the Greenland Sea and the Barents Sea
318 (Fig. 6b). The structure of the SST anomalies in the northwest Pacific is similar to that in Fig. 6a, but
319 with much smaller magnitude. Figure 6c, which shows the difference between these two anomalies
320 plots, further highlights the distribution of SST anomalies that are associated with more persistent haze
321 days: a prominent north–south tripolar mode over the North Atlantic and negative SST anomalies over
322 the Greenland Sea and Barents Sea.

323 SIC anomalies in the Greenland Sea and Barents–Kara Sea also show significant differences
324 between winters with the greatest number of persistent haze days and winters with the lowest number
325 of persistent haze days (Fig. 6d–f). The Greenland Sea and the southern part of the Barents Sea are
326 dominated by positive SIC anomalies and the Kara Sea shows negative SIC anomalies, though they
327 are not significant (Fig. 6d). The only positive SIC anomalies that differ significantly from zero are
328 found in the north of the Barents–Kara Sea and the southeast of Greenland (Fig. 6d). By contrast, for
329 the lowest number of hazy days composite significant negative SIC anomalies are located in the
330 Greenland Sea and the south part of the Barents Sea (Fig. 6e). The difference between Figures 6d and
331 6e also suggests that the decrease in sea ice in the Greenland Sea and the southern Barents Sea is not
332 conducive to a greater number of persistent haze days or haze events (Fig. 6f).

https://doi.org/10.5194/acp-2020-823
Preprint. Discussion started: 14 January 2021


Atmospheric Chemistry and Physics Discussions

From the composite analyses above, we can see that SST anomalies in the North Atlantic and SIC anomalies in the Greenland Sea and Barents–Kara Sea are associated with the occurrence of persistent haze days or haze events. To examine the potential causalities here we analyzed the composite SST anomalies and SIC anomalies averaged the period of 10 days prior to the first day of the 65 haze events. Prior to the persistent haze events, SST anomalies exhibit a north–south tripolar mode in the North Atlantic (Fig. 7a). This pattern differs from that shown in Fig. 6a; the tripolar mode is located further south, and has significant positive anomalies around the Florida peninsula and even into the Caribbean Sea, and significant negative SST anomalies off the northeast coast of the US (Fig. 7a). Figure 7a also shows significant negative SST anomalies in the Greenland Sea, and the Barents–Kara Sea. Turning to the SIC composite anomalies for these 65 events, we observe significant increases in the Greenland Sea and the Barents–Kara Sea (Fig. 7b). These prior distributions of SST and SIC anomalies are conducive to setting up the atmospheric circulations and zonal winds that are favorable for the formation of persistent Beijing haze events. The SST tripolar mode in the North Atlantic is favorable for the formation of an NAO+ pattern, and the strongly increased zonal wind in association with the NAO+ pattern encourages downstream wave train propagation. In concert with this, the decreased SST and increased SIC in the Barents–Kara Sea region potentially enables a strengthening of the cyclone upstream of the anticyclone over northern China, which is an essential part of the downstream wave train. Furthermore, as in Fig. 6a, the significant negative SST anomalies in the northwestern Pacific are not compatible with the anticyclone directly controlling persistent haze events in Beijing.

5 Relationship between persistent haze events and the preceding phase of the NAO pattern

The above analysis demonstrates that persistent haze weather in Beijing is closely related to the NAO+ pattern, in that the regression pattern in Fig. 1b resembles an NAO+ pattern with a downstream

https://doi.org/10.5194/acp-2020-823
Preprint. Discussion started: 14 January 2021


Atmospheric Chemistry and Physics Discussions

355 wave train more than an EA/WR+ pattern. Also, the NAO index has a stronger relationship with winter
356 haze days in Beijing than the EA/WR index, especially after 1999. More importantly, the NAO+
357 pattern leads the Day 0 of persistent haze events by 8–10 days, and corresponding SST signals could
358 be identified in the North Atlantic. Thus, the NAO+ pattern and related increased zonal winds and SST
359 anomalies are essential to the formation of persistent haze events in Beijing. We also note that SST
360 anomalies show opposite tripolar modes in Fig. 6a and Fig. 6b, meaning that the opposite SST mode
361 is unfavorable to the occurrence of persistent haze events in Beijing. This structure could force an
362 NAO− pattern through the air–sea interaction (Peng et al., 2002, 2003; Frankignoul and Kestenare,
363 2005; Luo et al., 2016; Jing et al., 2019).

364 In light of the above, we comment that, even though regression and composite analyses (e.g., Fig.
365 1) might suggest a strong link between haze events and the NAO+, it is important to remember that
366 such analyses identify *necessary* but not *sufficient* conditions (see Boschat et al., 2016). This leads us
367 to the question as to whether there are persistent haze events related to the NAO− pattern and what the
368 differences are between these haze events and those related to the NAO+ pattern. First, the daily
369 evolutions of the NAO index for the 65 persistent haze events (black line), 43 NAO+-related persistent
370 haze events (red line) and 22 NAO−-related persistent haze events (green line) are shown in Fig. 8.
371 The composite NAO index for all haze events reaches its highest value on Day −8, which is consistent
372 with Fig. 3 where the NAO+ pattern is more prominent from Day −10 to Day −8. Thus, we select the
373 NAO+-related (NAO−-related) persistent haze event if its averaged NAO index during the period of
374 Day −10 to Day −6 is above (below) zero. As shown in Fig. 8, the daily evolution of the composite
375 NAO index for NAO+-related and NAO−-related persistent haze events generally shows the opposite
376 character. However, the peak value (0.90) of the NAO index for NAO+-related persistent haze events

https://doi.org/10.5194/acp-2020-823
Preprint. Discussion started: 14 January 2021


Atmospheric Chemistry and Physics Discussions

377 also appears on Day −8, whose absolute value is larger than that of the valley value (−0.68) of the
378 NAO index for NAO−-related persistent haze events on Day −10. Corresponding SST and SIC
379 anomalies of the NAO+-related case and the NAO−-related case are also compared in Figures 8b–8d.
380 We use a difference in the SST anomalies between the two regions A (40° N–55° N, 70° W–20° W)
381 and B (22° N–37° N, 85° W–35° W) marked in Fig. 7a to signify the SST tripolar pattern in the
382 North Atlantic, which could be related to an NAO+ pattern. Daily evolutions of the SST anomaly
383 difference show significant increases starting from Day −11 and Day −9 for the NAO+-related case
384 and all persistent haze events, respectively, whereas the difference in SST anomalies for the NAO−-
385 related case shows only a weak fluctuation (Fig. 8b). As for the SIC anomaly in the Barents–Kara Sea,
386 it has a significant maximum amplitude leading the Day 0 of NAO+-related persistent haze events by
387 12 days (Fig. 8d), while the SIC anomaly in the Greenland Sea shows significant high values during
388 the period from Day −15 to Day 15 of NAO−-related persistent haze events and its peak appears on
389 Day −3 (Fig. 8c). Thus, we can conclude that the SST anomalies in the North Atlantic and SIC
390 anomalies in the Barents–Kara Sea show preceding signals for NAO+-related persistent haze events,
391 and the NAO−-related persistent haze events are associated mainly with increased SIC anomalies in
392 the Greenland Sea.

393 Furthermore, a comparison between the evolution of atmospheric circulations for persistent haze
394 events related to the NAO+ pattern and the NAO− pattern is made in Fig. 9. For the NAO+-related
395 case, the development of atmospheric circulation is similar to that in Fig. 3, while the NAO+ pattern
396 is more prominent (Fig. 9a). Moreover, the persistent NAO+ pattern over the North Atlantic
397 corresponds to the significantly strengthened dipole mode in the SST, as suggested in Fig. 8b, which
398 sustains the propagation of the wave train; and the increased SIC (increased SST) in the Barents–Kara

https://doi.org/10.5194/acp-2020-823
Preprint. Discussion started: 14 January 2021


Atmospheric Chemistry and Physics Discussions

399 Sea could affect the cyclone over Siberia, a node of the wave train. In Fig. 9b, the NAO− pattern is
400 situated over the North Atlantic on Day −6, whose north anticyclone corresponds to the increased SIC
401 anomalies at the Greenland Sea. The wave activity originates mainly from the north center of the
402 NAO− pattern (Day −6). As the wave activity flux propagates downstream, an anticyclone forms over
403 northeastern China on Day −2 and reaches its greatest intensity on Day 0. Compared with the evolution
404 of the wave train in Fig. 9a, that in Fig. 9b has a longer wavelength, but it is less organized and less
405 persistent. This suggests that the preceding NAO+ pattern could increase the occurrence of persistent
406 haze events compared to the NAO− pattern.

407 To confirm the role of the NAO+ pattern in the occurrence of persistent haze weather in Beijing,
408 we also compare the number of persistent haze days and persistent haze events that occur in NAO+
409 winters and NAO− winters. The NAO+ winters (NAO− winters) are classified with four sets of criteria
410 to make our results more solid and convincing. If the normalized NAO index of DJF is above the
411 50th/75th/90th/95th percentile (below the 50th/25th/10th/5th percentile), NAO+ winters (NAO−
412 winters) are selected. It is found that the number of persistent haze days and persistent haze events
413 happening in NAO+ winters are much larger than in NAO− winters (Fig. 10). The discrepancy is
414 especially large for the 90th (10th) and 75th (25th) percentiles. For these two sets of criteria, the
415 number of hazy days in NAO+ winters is more than twice that in NAO− winters, while the number of
416 haze events in NAO+ winters is nearly double that in NAO− winters. This also suggests that the haze
417 events in NAO+ winters have longer durations. Though the differences in the number of persistent
418 haze days (events) for the 95th (5th) and 50th (50th) percentiles, which contain the lowest number of
419 haze days (events) and the greatest number of haze days (events), are not as apparent as the other two
420 sets of criteria, NAO+ winters still have a greater number of persistent haze days (events). This

https://doi.org/10.5194/acp-2020-823
Preprint. Discussion started: 14 January 2021


Atmospheric Chemistry and Physics Discussions

421 confirms our finding that the NAO+ pattern is more conducive to the occurrence of persistent haze
422 weather in Beijing.

423 **6 Conclusions and discussions**

424 In this study, we have focused mainly on persistent winter haze events in Beijing from the
425 perspective of large-scale atmospheric circulation (e.g., teleconnections and wave train). We first
426 presented the atmospheric circulation correlated with winter haze days in Beijing on interannual
427 timescales. It is consistent with previous studies that an NAO+ pattern and an EA/WR+ pattern are
428 related to the frequency of winter haze (Yin et al. 2017; Yin and Wang, 2017; Chen et al. 2019).
429 Furthermore, our new result shows that the NAO+ pattern has a stronger relationship with winter haze
430 days, especially after 1999. In addition, the NAO+ index corresponds better to the winters with the
431 greatest and lowest number of hazy days.

432 To increase our understanding of the relationship between winter haze weather in Beijing and
433 atmospheric circulation, we investigated the daily evolution of the composite circulation patterns and
434 wave activities for 65 persistent haze events. A transmission of atmospheric circulation demonstrated
435 a wave train propagating from the North Atlantic to northeast China. The NAO+ pattern performs as
436 the origin of this transmission from Day −10 to Day −8, followed by an EA/WR+ pattern from Day
437 −3 to Day −2. We also highlighted the daily variations in zonal winds linked to atmospheric circulation.
438 It was revealed that the zonal wind over the central North Atlantic, which is coupled with the NAO+
439 pattern, reached its largest value on Day −9, and the zonal wind downstream over the Scandinavian
440 Peninsula and the north of China showed significantly increased values after Day −5, indicating the
441 propagation of the wave train. Thus, the NAO+ pattern and the downstream wave train, as well as the
442 successive increases in zonal winds could serve as potential predictors for persistent winter haze events

https://doi.org/10.5194/acp-2020-823
Preprint. Discussion started: 14 January 2021


Atmospheric Chemistry and Physics Discussions

443 in Beijing.

444 It should be noted that the last node of the wave train is an anticyclone over northeastern China,
445 which is directly associated with the formation of haze over Beijing (Zhong et al., 2019). We then
446 investigated the local meteorological conditions associated with the anticyclone that are conducive to
447 the accumulation of haze pollutants over Beijing. The negative anomalous pressure over mainland
448 China and the positive anomalous pressure over the coastal regions suggest a weakened EAWM.
449 Correspondingly, there are southerly winds and decreased wind speed in Beijing. Furthermore, the
450 BLH decreases, while A_I increases during the haze episodes. These conditions can suppress the
451 ventilation and dispersal of haze pollutants. In addition, the anomalously high values of relative
452 humidity and temperature at 925 hPa could worsen the hazy weather by accelerating the hydroscopic
453 growth of pollutants. However, these meteorological conditions show almost simultaneous variations
454 with the process of persistent haze events; thus, it is difficult to use them as predictors.

455 Atmospheric circulations can be forced by external influences and these, in turn, may provide
456 precursors to haze events. Analyses revealed that the SST anomalies in the North Atlantic and SIC
457 anomalies in the Greenland Sea and Barents–Kara Sea are related to winter haze weather in Beijing on
458 both interannual and intra-seasonal timescales. On interannual timescales, winters with a greater
459 number of persistent haze days correspond to a north–south tripolar mode over the North Atlantic. On
460 intra-seasonal timescales, a more southerly SST tripolar mode is also prominent over the North Atlantic,
461 and the Greenland Sea and Barents–Kara Sea also present significant SST and SIC anomalies 10 days
462 prior to the persistent haze events. For a more in-depth understanding, the relationship between the
463 preceding NAO pattern, SST and SIC anomalies and the persistent haze events was highlighted by a
464 comparison of NAO+-related haze events and NAO−-related events. We found that the NAO+-related

https://doi.org/10.5194/acp-2020-823
Preprint. Discussion started: 14 January 2021


Atmospheric Chemistry and Physics Discussions

case corresponds to prior SST signals in the North Atlantic and increased SIC anomalies in the Barents–Kara Sea, while the NAO−-related case had large SIC anomalies only in the Greenland Sea. We proposed that these SST and SIC anomalies could also provide hints for the prediction of persistent haze events in Beijing, especially for the NAO+-related case, considering that the SST tripolar mode in the North Atlantic can affect the NAO+ pattern and the change in the SST and SIC at the Barents–Kara Sea promotes the downstream propagation of the wave train.

It has also been revealed that the number of NAO+-related haze events is nearly double the number of the NAO−-related cases, and the atmospheric circulation and the propagation of wave activity are more organized for the NAO+-related case. These results indicate that persistent haze events are more likely to occur with the NAO+ pattern. To verify this proposition, we further compared the number of persistent haze days and persistent haze events in NAO+ winters and NAO− winters with four sets of criteria. It was found that the numbers of both haze days and haze events are larger in NAO+ winters, especially for the 95th (5th) and 50th (50th) percentiles.

SSTs in the Atlantic (Xiao et al. 2015; Wang et al. 2019), SICs in the Arctic (Wang and Zhang, 2015; Yin et al. 2019a, 2019b) as well as the large-scale atmospheric circulations (Yin and Wang 2017; Yin et al. 2017; Chen et al. 2019) have been pointed out to be closely associated with the winter haze in Beijing from decadal timescales down to intra-seasonal timescales. These studies well captured certain modes of SSTs, SICs and atmospheric circulations that are significant during the haze episodes, but did not reveal their lead-lag relationships on daily time scales. Through analyzing the day-by-day evolutions, our investigation has revealed that the NAO+ pattern, part of an atmospheric transmission, and the associated intensified zonal wind, SST mode and SIC anomalies show potential prediction abilities for persistent haze events, which provides us with a possible approach for the prediction of

https://doi.org/10.5194/acp-2020-823
Preprint. Discussion started: 14 January 2021


Atmospheric Chemistry and Physics Discussions

winter haze weather in Beijing. The preceding signals in the SST, SIC and atmospheric transmission over the North Atlantic and Eurasia may serve as a predictor for persistent haze events. In further studies, it will be necessary to qualitatively estimate the contributions of emissions and atmospheric transmission patterns in haze formation. This could be useful for the government to take effective measures to reduce emissions, to reduce the occurrence of the winter haze weather in Beijing. In addition, it is also worthwhile figuring out the reasons why the NAO index (EA/WR index) has a stronger correlation with winter haze weather in Beijing after 1999 (before 2000) from the perspective of climate change.

Data availability. Daily atmospheric and land-surface data were downloaded from the ECMWF ERA-Interim data archive (http://www.ecmwf.int/en/research/climate-reanalysis/era-interim) (ERA-Interim, 2017). Monthly sea surface temperature data and sea ice concentration data are available from the Met Office Hadley Centre datasets (https://www.metoffice.gov.uk/hadobs/hadisst/data/download.html) (Met Office, 2017). The ground observations were taken from the National Meteorological Information Center of China (http://data.cma.cn/) (CMA, 2017). The NAO and EA/WR indices are from the NOAA's Climate Prediction Center (http://www.cpc.ncep.noaa.gov/data/teledoc/telecontents.shtml) (CPC, 2017). The modified LW03 NAO index can be obtained from the authors.

Competing interests. The authors declare that they have no conflict of interest.

Author contributions. YY designed the study. ML created the figures. ML and YY wrote the manuscript. IS, DL and LZ gave constructive comments. LP provided and analyzed the observational

https://doi.org/10.5194/acp-2020-823
Preprint. Discussion started: 14 January 2021


Atmospheric Chemistry and Physics Discussions

509 station data.

510

511 ***Acknowledgments.*** The authors acknowledge support from the National Natural Science Foundation
512 of China (Grants 41975068 and 41790473) and the National Key Research and Development Program
513 of China (Grant 2016YFA0601802). Simmonds was supported by Australian Research Council Grant
514 DP16010997.

515 **References**:

516 Ambrizzi, T., Hoskins, B. J., and Hsu, H. H.: Rossby-wave propagation and teleconnection patterns in
517 the austral winter, J. Atmos. Sci., 52, 3661–3672, doi:10.1175/1520-
518 0469(1995)052<3661:rwpatp>2.0.co;2, 1995.
519 An, Z., Huang, R. J., Zhang, R., Tie, X., Li, G., Cao, J., Zhou, W., Shi, Z., Han, Y., Gu, Z., and Ji, Y.:
520 Severe haze in northern China: A synergy of anthropogenic emissions and atmospheric processes, P.
521 Natl. Acad. Sci. USA, 116, 8657–8666, doi:10.1073/pnas.1900125116, 2019.
522 Athanasiadis, P. J., Wallace, J. M., and Wettstein, J. J.: Patterns of wintertime jet stream variability and
523 their relation to the storm tracks, J. Atmos. Sci., 67, 1361–1381, doi:10.1175/2009jas3270.1, 2010.
524 Barnston, A. G., and Livezey, R. E.: Classification, seasonality and persistence of low-frequency
525 atmospheric circulation patterns, Mon. Weather Rev., 115, 1083–1126, doi:10.1175/1520-
526 0493(1987)115<1083:csapol>2.0.co;2, 1987.
527 Boschat, G., Simmonds, I., Purich, A., Cowan, T., and Pezza, A. B.: On the use of composite analyses
528 to form physical hypotheses: An example from heat wave - SST associations, Sci. Rep., 6, 9,
529 doi:10.1038/srep29599, 2016.
530 Chang, L., Wu, Z., and Xu, J.: A comparison of haze pollution variability in China using haze indices

https://doi.org/10.5194/acp-2020-823
Preprint. Discussion started: 14 January 2021


Atmospheric Chemistry and Physics Discussions

531 based on observations, Sci. Total Environ., 715, doi:10.1016/j.scitotenv.2020.136929, 2020.
532 Chen, H., and Wang, H.: Haze days in North China and the associated atmospheric circulations based
533 on daily visibility data from 1960 to 2012, J. Geophys. Res.-Atmos., 120, 5895–5909,
534 doi:10.1002/2015jd023225, 2015.
535 Chen, S., Guo, J., Song, L., Li, J., Liu, L., and Cohen, J. B.: Inter-annual variation of the spring haze
536 pollution over the North China Plain: Roles of atmospheric circulation and sea surface temperature,
537 Int. J. Climatol., 39, 783–798, doi:10.1002/joc.5842, 2019.
538 Chen, S., Guo, J., Song, L., Cohen, J. B., and Wang, Y.: Temporal disparity of the atmospheric systems
539 contributing to interannual variation of wintertime haze pollution in the North China Plain, Int. J.
540 Climatol., 40, 128–144, doi:10.1002/joc.6198, 2020a.
541 Chen, S., Guo, J., Song, L., Cohen, J. B. and Wang, Y.: Intra-seasonal differences in the atmospheric
542 systems contributing to interannual variations of autumn haze pollution in the North China Plain,
543 Theor. Appl. Climatol., 141, 389–403, doi: 10.1007/s00704-020-03221-4, 2020b.
544 China Meteorological Administration. Specifications for surface meteorological observation. Beijing:
545 China Meteorological Press, 129–130, 2004.
546 Dang, R., and Liao, H.: Severe winter haze days in the Beijing-Tianjin-Hebei region from 1985 to
547 2017 and the roles of anthropogenic emissions and meteorology, Atmos. Chem. Phys., 19, 10801–
548 10816, doi:10.5194/acp-19-10801-2019, 2019.
549 Dee, D. P., et al.: The ERA-Interim reanalysis: configuration and performance of the data assimilation
550 system, Q. J. Roy. Meteor. Soc., 137, 553–597, doi:10.1002/qj.828, 2011.
551 Fang, Z. F., Wallace, J. M., and Thompson, D. W. J.: The relationship between the meridional profile
552 of zonal-mean geostrophic wind and station wave at 500 hPa, Adv. Atmos. Sci., 18, 692–700,

https://doi.org/10.5194/acp-2020-823
Preprint. Discussion started: 14 January 2021

553 doi:10.1007/BF03403494, 2001.

554 Frankignoul, C., and Kestenare, E.: Observed Atlantic SST anomaly impact on the NAO: An update,
555 J. Climate, 18, 4089–4094, doi:10.1175/jcli3523.1, 2005.

556 He, J., Gong, S., Zhou, C., Lu, S., Wu, L., Chen, Y., Yu, Y., Zhao, S., Yu, L., and Yin, C.: Analyses of
557 winter circulation types and their impacts on haze pollution in Beijing, Atmos. Environ., 192, 94–
558 103, doi:10.1016/j.atmosenv.2018.08.060, 2018.

559 Jing, Y. J., Li, Y. C., Xu, Y. F., and Fan, G. Z.: Influences of different definitions of the winter NAO
560 index on NAO action centers and its relationship with SST, Atmos. Ocean. Sci. Lett., 12, 320–328,
561 doi:10.1080/16742834.2019.1628607, 2019.

562 Li, J., and Han, Z.: A modeling study of severe winter haze events in Beijing and its neighboring
563 regions, Atmos. Res., 170, 87–97, doi:10.1016/j.atmosres.2015.11.009, 2016.

564 Li, J., Du, H., Wang, Z., Sun, Y., Yang, W., Li, J., Tang, X., and Fu, P.: Rapid formation of a severe
565 regional winter haze episode over a mega-city cluster on the North China Plain, Environ. Pollut.,
566 223, 605–615, doi:10.1016/j.envpol.2017.01.063, 2017.

567 Li, J., Sun, J., Zhou, M., Cheng, Z., Li, Q., Cao, X., and Zhang, J.: Observational analyses of dramatic
568 developments of a severe air pollution event in the Beijing area, Atmos. Chem. Phys., 18, 3919–
569 3935, doi:10.5194/acp-18-3919-2018, 2018a.

570 Li, K., Liao, H., Cai, W., and Yang, Y.: Attribution of anthropogenic influence on atmospheric patterns
571 conducive to recent most severe haze over Eastern China, Geophys. Res. Lett., 45, 2072–2081,
572 doi:10.1002/2017gl076570, 2018b.

573 Li, J. P., and Wang, J. X. L.: A new North Atlantic Oscillation index and its variability, Adv. Atmos.
574 Sci., 20, 661–676, doi:10.1007/BF02915394, 2003.

https://doi.org/10.5194/acp-2020-823
Preprint. Discussion started: 14 January 2021


Atmospheric Chemistry and Physics Discussions

575 Li, X., Gao, Z., Li, Y., Gao, C. Y., Ren, J., and Zhang, X.: Meteorological conditions for severe foggy
576 haze episodes over north China in 2016-2017 winter, Atmos. Environ., 199, 284–298,
577 doi:10.1016/j.atmosenv.2018.11.042, 2019.
578 Li, Y., and Yin, Z.: Melting of Perennial Sea Ice in the Beaufort Sea Enhanced Its Impacts on Early-
579 Winter Haze Pollution in North China after the Mid-1990s, J. Climate, 33, 5061–5080,
580 doi:10.1175/jcli-d-19-0694.1, 2020.
581 Lu, S., He, J., Gong, S., and Zhang, L.: Influence of Arctic Oscillation abnormalities on spatio-
582 temporal haze distributions in China, Atmos. Environ., 223, doi:10.1016/j.atmosenv.2020.117282,
583 2020.
584 Luo, D., Xiao, Y., Yao, Y., Dai, A., Simmonds, I., and Franzke, C. L. E.: Impact of Ural blocking on
585 winter warm Arctic-cold Eurasian anomalies. Part I: Blocking-induced amplification, J. Climate, 29,
586 3925–3947, doi:10.1175/jcli-d-15-0611.1, 2016.
587 Luo D., Yao, Y., and Feldstein, S.: Regime transition of the North Atlantic Oscillation and the extreme
588 cold event over Europe in January-February 2012, Mon. Wea. Rev., 142, 4735-4757,
589 doi:10.1175/MWR-D-13-00234.1, 2014.
590 Martinez-Asensio, A., Tsimplis, M. N., Marcos, M., Feng, X., Gomis, D., Jorda, G., and Josey, S. A.:
591 Response of the North Atlantic wave climate to atmospheric modes of variability, Int. J. Climatol.,
592 36, 1210–1225, doi:10.1002/joc.4415, 2016.
593 Pei, L., and Yan, Z.: Diminishing clear winter skies in Beijing towards a possible future, Environ. Res.
594 Lett., 13 (12), 124029, doi:10.1088/1748-9326/aaf032, 2018.
595 Pei, L., Yan, Z., Sun, Z., Miao, S., and Yao, Y.: Increasing persistent haze in Beijing: potential impacts
596 of weakening East Asian winter monsoons associated with northwestern Pacific sea surface

https://doi.org/10.5194/acp-2020-823
Preprint. Discussion started: 14 January 2021


Atmospheric Chemistry and Physics Discussions

temperature trends, Atmos. Chem. Phys., 18, 3173–3183, doi:10.5194/acp-18-3173-2018, 2018.

Pei, L., Yan, Z., Chen, D., and Miao, S.: Climate variability or anthropogenic emissions: which caused Beijing Haze? Environ. Res. Lett., 15 (3), 034004, doi:10.1088/1748-9326/ab6f11, 2020.

Peng, S. L., Robinson, W. A., and Li, S. L.: North Atlantic SST forcing of the NAO and relationships with intrinsic hemispheric variability, Geophys. Res. Lett., 29 (8), 1276, doi:10.1029/2001gl014043, 2002.

Peng, S. L., Robinson, W. A., and Li, S. L.: Mechanisms for the NAO responses to the North Atlantic SST tripole, J. Climate, 16, 1987–2004, doi:10.1175/1520-0442(2003)016<1987:mftnrt>2.0.co;2, 2003.

Rayner, N. A., Parker, D. E., Horton, E. B., Folland, C. K., Alexander, L. V., Rowell, D. P., Kent, E. C., and Kaplan, A.: Global analyses of sea surface temperature, sea ice, and night marine air temperature since the late nineteenth century, J. Geophys. Res.-Atmos., 108 (D14), 4407, doi:10.1029/2002jd002670, 2003.

Shi, P., Zhang, G., Kong, F., Chen, D., Azorin-Molina, C., and Guijarro, J. A.: Variability of winter haze over the Beijing-Tianjin-Hebei region tied to wind speed in the lower troposphere and particulate sources, Atmos. Res., 215, 1–11, doi:10.1016/j.atmosres.2018.08.013, 2019.

Simmonds, I., and Govekar, P. D.: What are the physical links between Arctic sea ice loss and Eurasian winter climate?, Environ. Res. Lett., 9 (10), 101003, doi:10.1088/1748-9326/9/10/101003, 2014.

Su, B., Zhan, M., Zhai, J., Wang, Y., and Fischer, T.: Spatio-temporal variation of haze days and atmospheric circulation pattern in China (1961-2013), Quat. Int., 380, 14–21, doi:10.1016/j.quaint.2014.11.044, 2015.

Takaya, K., and Nakamura, H.: A formulation of a phase-independent wave-activity flux for stationary

https://doi.org/10.5194/acp-2020-823
Preprint. Discussion started: 14 January 2021


Atmospheric Chemistry and Physics Discussions

and migratory quasigeostrophic eddies on a zonally varying basic flow, J. Atmos. Sci., 58, 608–627, doi:10.1175/1520-0469(2001)058<0608:afoapi>2.0.co;2, 2001.

Wang, H., Xu, J., Zhang, M., Yang, Y., Shen, X., Wang, Y., Chen, D., and Guo, J.: A study of the meteorological causes of a prolonged and severe haze episode in January 2013 over central-eastern China, Atmos. Environ., 98, 146–157, doi:10.1016/j.atmosenv.2014.08.053, 2014.

Wang, H. J., Chen, H. P., and Liu, J. P.: Arctic Sea Ice Decline Intensified Haze Pollution in Eastern China, Atmos. Ocean. Sci. Lett., 8, 1–9, doi:10.3878/AOSL20140081, 2015.

Wang, H., Li, J. H., Peng, Y., Zhang, M., Che, H. Z., and Zhang, X. Y.: The impacts of the meteorology features on PM2.5 levels during a severe haze episode in central-east China, Atmos. Environ., 197, 177–189, doi:10.1016/j.atmosenv.2018.10.001, 2019.

Wang, N., and Zhang, Y. C.: Connections between the Eurasian teleconnection and concurrent variation of upper-level jets over East Asia, Adv. Atmos. Sci., 32, 336–348, doi:10.1007/s00376-014-4088-1, 2015.

Wang, J., Zhu, Z., Qi, L., Zhao, Q., He, J., and Wang, J. X. L.: Two pathways of how remote SST anomalies drive the interannual variability of autumnal haze days in the Beijing-Tianjin-Hebei region, China, Atmos. Chem. Phys., 19, 1521–1535, doi:10.5194/acp-19-1521-2019, 2019.

Wang, J., Liu, Y., Ding, Y., Wu, P., Zhu, Z., Xu, Y., Li, Q., Zhang, Y., He, J., Wang, J. X. L., and Qi, L.: Impacts of climate anomalies on the interannual and interdecadal variability of autumn and winter haze in North China: A review, International Journal of Climatology, 10.1002/joc.6471, 2020.

Wang, Y. S., Yao, L., Liu, Z. R., J., D. S., Wang, L. L., and Zhang, J. K.: Formation mechanism and control strategies of haze in China (in Chinese), Bull. Chin. Acad. Sci., 28, 353–363, 2013.

Wirth, V., Riemer, M., Chang, E. K. M., and Martius, O.: Rossby Wave Packets on the Midlatitude

https://doi.org/10.5194/acp-2020-823
Preprint. Discussion started: 14 January 2021


Atmospheric Chemistry and Physics Discussions

641 Waveguide-A Review, Mon. Weather Rev., 146, 1965–2001, doi:10.1175/mwr-d-16-0483.1, 2018.
642 Wu, D.: More Discussions on the differences between Haze and Fog in City, Quat. Int., 32, 9–15, 2006.
643 Wu D.: Discussion on the distinction between haze and fog and analysis and processing of data,
644 Environ. Chem., 27(3): 327–330, 2008.
645 Wu, P., Ding, Y., and Liu, Y.: Atmospheric circulation and dynamic mechanism for persistent haze
646 events in the Beijing-Tianjin-Hebei region, Adv. Atmos. Sci., 34, 429–440, doi:10.1007/s00376-
647 016-6158-z, 2017.
648 Wu, Y., Zhang, R., Tian, P., Tao, J., Hsu, S. C., Yan, P., Wang, Q., Cao, J., Zhang, X., and Xia, X.:
649 Effect of ambient humidity on the light absorption amplification of black carbon in Beijing during
650 January 2013, Atmos. Environ., 124, 217–223, doi:10.1016/j.atmosenv.2015.04.041, 2016.
651 Xiao, D., Li, Y., Fan, S., Zhang, R., Sun, J., and Wang, Y.: Plausible influence of Atlantic Ocean SST
652 anomalies on winter haze in China, Theor. Appl. Climatol., 122, 249–257, doi:10.1007/s00704-014-
653 1297-6, 2015.
654 Yang, Y., Liao, H., and Lou, S.: Increase in winter haze over eastern China in recent decades: Roles of
655 variations in meteorological parameters and anthropogenic emissions, J. Geophys. Res.-Atmos., 121,
656 13050–13065, doi:10.1002/2016jd025136, 2016.
657 Yao, Y., Luo, D., Dai, A. and Feldstein, S.: The positive North Atlantic Oscillation with downstream
658 blocking and Middle East snowstorms: Impacts of the North Atlantic jet, J. Climate., 29, 1853–1876,
659 doi:10.1175/JCLI-D-15-0350.1, 2016.
660 Yao Y., and Luo, D.: Relationship between zonal position of the North Atlantic Oscillation and Euro-
661 Atlantic blocking events and its possible effect on the weather over Europe. Sci. China. Earth. Sci.,
662 57, 2628–2636, doi:10.1007/s11430-014-4949-6, 2014.

https://doi.org/10.5194/acp-2020-823
Preprint. Discussion started: 14 January 2021


Atmospheric Chemistry and Physics Discussions

663 Yin, Z., and Wang, H.: Role of atmospheric circulations in haze pollution in December 2016, Atmos.
664 Chem. Phys., 17, 11673–11681, doi:10.5194/acp-17-11673-2017, 2017.
665 Yin, Z., Wang, H., and Che, H.: Understanding severe winter haze events in the North China Plain in
666 2014: roles of climate anomalies, Atmos. Chem. Phys., 17, 1642–1652, doi:10.5194/acp-17-1641-
667 2017, 2017.
668 Yin, Z., Li, Y., and Wang, H.: Response of early winter haze in the North China Plain to autumn
669 Beaufort sea ice, Atmos. Chem. Phys., 19, 1439-1453, doi:10.5194/acp-19-1439-2019, 2019a.
670 Yin, Z., Wang, H., and Ma, X.: Possible Relationship between the Chukchi Sea Ice in the Early Winter
671 and the February Haze Pollution in the North China Plain, J. Climate, 32, 5179–5190,
672 doi:10.1175/jcli-d-18-0634.1, 2019b.
673 Zhang, G. C., Jiao, M. Y., Li, Y. X.: Techniques and methods of contemporary weather forecast (in
674 Chinese). Beijing: China, Meteorological Press. 371, 2007.
675 Zhang, R., Li, Q., and Zhang, R.: Meteorological conditions for the persistent severe fog and haze
676 event over eastern China in January 2013, Sci. China Earth Sci., 57, 26–35, doi:10.1007/s11430-
677 013-4774-3, 2014.
678 Zhang, Y., Fan, J., Chen, X., Ashkenazy, Y., and Havlin, S.: Significant Impact of Rossby Waves on
679 Air Pollution Detected by Network Analysis, Geophys. Res. Lett., 46, 12476–12485,
680 doi:10.1029/2019gl084649, 2019.
681 Zhang, Z., Zhang, X., Gong, D., Kim, S. J., Mao, R., and Zhao, X.: Possible influence of atmospheric
682 circulations on winter haze pollution in the Beijing-Tianjin-Hebei region, northern China, Atmos.
683 Chem. Phys., 16, 561–571, doi:10.5194/acp-16-561-2016, 2016.
684 Zhong, W., Yin, Z., and Wang, H.: The relationship between anticyclonic anomalies in northeastern

https://doi.org/10.5194/acp-2020-823
Preprint. Discussion started: 14 January 2021

Atmospheric Chemistry and Physics Discussions

685 Asia and severe haze in the Beijing-Tianjin-Hebei region, Atmos. Chem. Phys., 19, 5941–5957,
686 doi:10.5194/acp-19-5941-2019, 2019.
687 Zou, Y., Wang, Y., Zhang, Y., and Koo, J.-H.: Arctic sea ice, Eurasia snow, and extreme winter haze in
688 China, Sci. Adv., 3 (3), e1602751, doi:10.1126/sciadv.1602751, 2017.

689

690

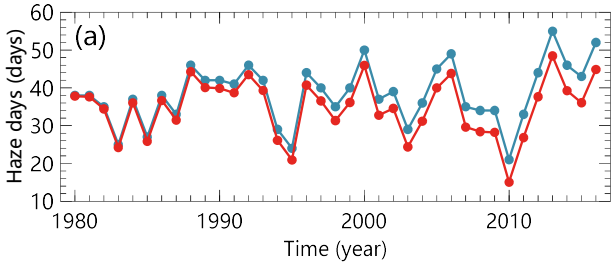

691

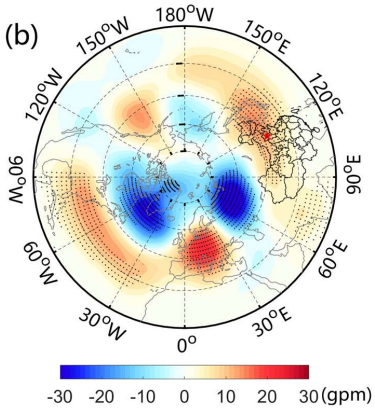

692

693 **Figure 1. (a)** Time series of winter haze days (blue) and detrended winter haze days (red) in Beijing
694 from 1980 to 2016. To aid visualization, a fixed value is added to all the detrended data so that the first
695 values of both series coincide. **(b)** Regressed Z500 anomalies (shading; units: gpm) against the
696 detrended winter haze days. The dotted areas show values that are above the 95% confidence level
697 based on the two-sided Student's *t*-test. For all plots in this study, the red star denotes the location of

https://doi.org/10.5194/acp-2020-823
Preprint. Discussion started: 14 January 2021

Atmospheric Chemistry and Physics Discussions

698 Beijing.

699

700

701

702

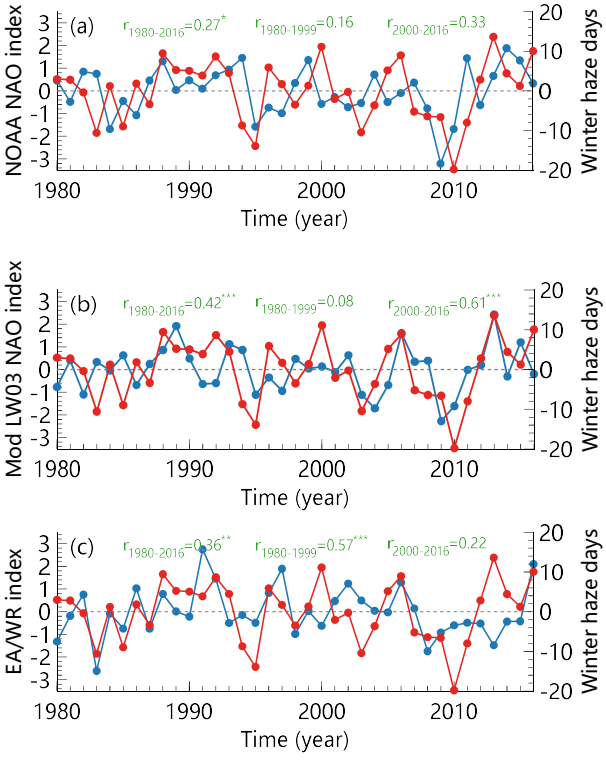

703

704

705

706 **Figure 2.** Time series of detrended winter haze days (red) and (a) NOAA NAO index (blue), (b)

707 modified LW03 NAO index (blue) and (c) NOAA EA/WR index (blue). Correlation coefficients

708 between winter haze days and the three indices during the periods 1980–2016, 1980–1999 and 2000–

709 2016 are labelled at the top of each panel. The 90%, 95% and 99% confidence levels for the Student's

710 *t*-test are denoted by one, two and three asterisks, respectively.

711

https://doi.org/10.5194/acp-2020-823
Preprint. Discussion started: 14 January 2021

Atmospheric Chemistry and Physics Discussions

712

713

714

715

716

717

718

719

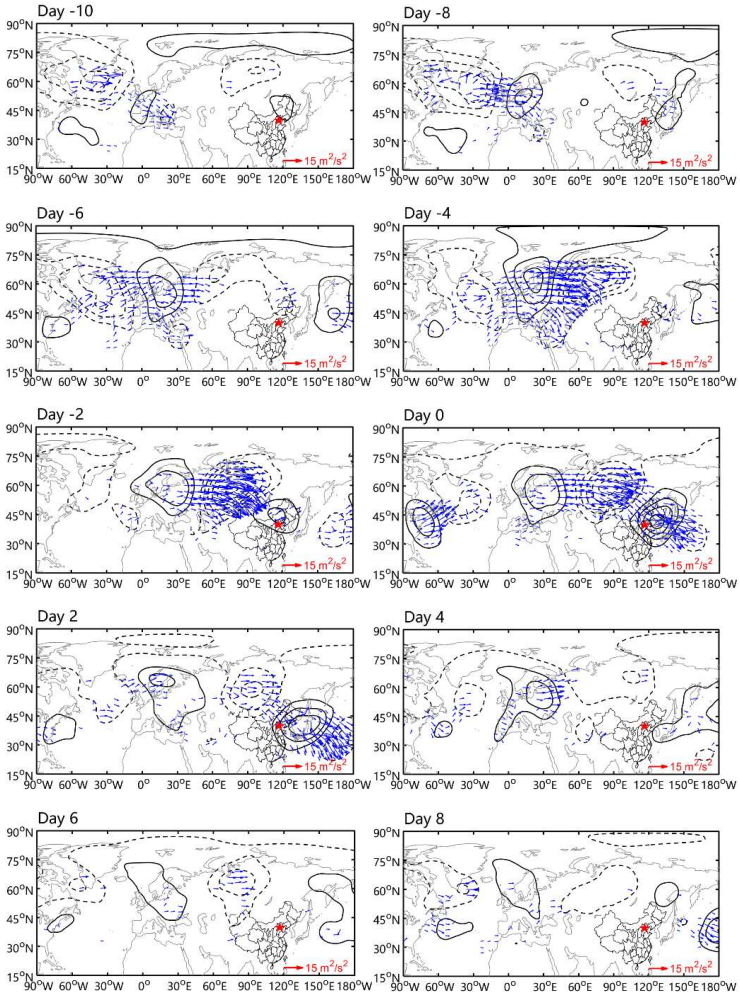

720 **Figure 3.** Instantaneous fields of the composite daily Z500 anomalies (contours, interval = 20; units:

721 gpm), and horizontal components of wave activity developed by Takaya and Nakamura (2001) (arrows;

722 units: m^2/s^2) from Day −10 to Day 8 for the 65 persistent haze events.

723

https://doi.org/10.5194/acp-2020-823
Preprint. Discussion started: 14 January 2021

Atmospheric Chemistry and Physics Discussions

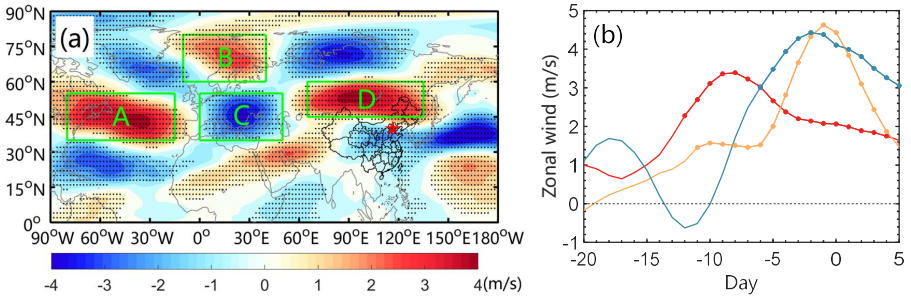

Figure 4. (a) Composite 300 hPa zonal wind anomalies (shading; units: m/s) between Day −10 and Day 5 for the 65 persistent haze events. The dotted areas show values that are above the 95% confidence level based on the two-sided Student's *t*-test. **(b)** Composite daily time series of region-averaged 300 hPa zonal wind anomalies in region A (80° W–15° W, 35° N–55° N) (red) and region D (65° E–135° E, 45° N–60° N) (orange) and the difference in region-averaged zonal wind anomalies between region B (10° W–40° E, 60° N–80° N) and region C (0° W–50° E, 35° N–55° N) (blue). The dots denote the days with values that are above the 95% confidence level for the two-sided Student's *t*-test.

https://doi.org/10.5194/acp-2020-823
Preprint. Discussion started: 14 January 2021

Atmospheric Chemistry and Physics Discussions

743

744

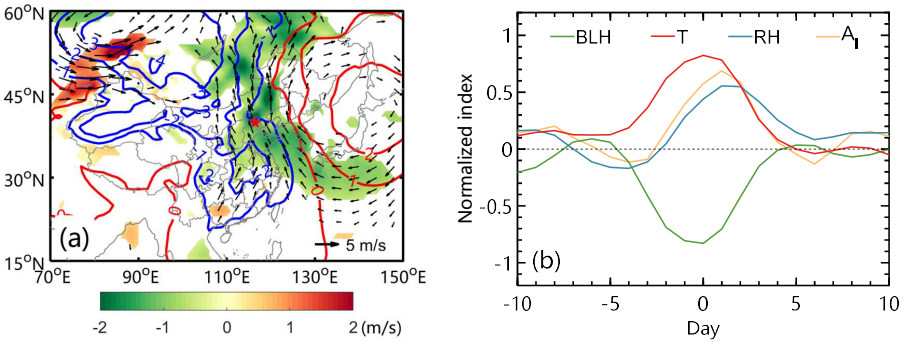

745

746 **Figure 5. (a)** Composite anomalous 850 hPa horizontal wind vector (vector), 850 hPa wind speed
747 (shading; units: m/s) and SLP (contour; units: hPa) between Day −2 and Day 2 for the 65 persistent
748 haze events. Only wind vectors above 1 m/s are plotted. **(b)** Composite daily time series of boundary
749 layer height (BLH, green), temperature (T, red), relative humidity (RH, blue) and A_I (yellow) at 925
750 hPa averaged over the region of Beijing (115° E–118° E, 39° N–42° N, marked with a red star in **(a)**)
751 for the 65 persistent haze events.

752

753

754

755

756

757

758

759

760

https://doi.org/10.5194/acp-2020-823
Preprint. Discussion started: 14 January 2021

Atmospheric Chemistry and Physics Discussions

761

762

763

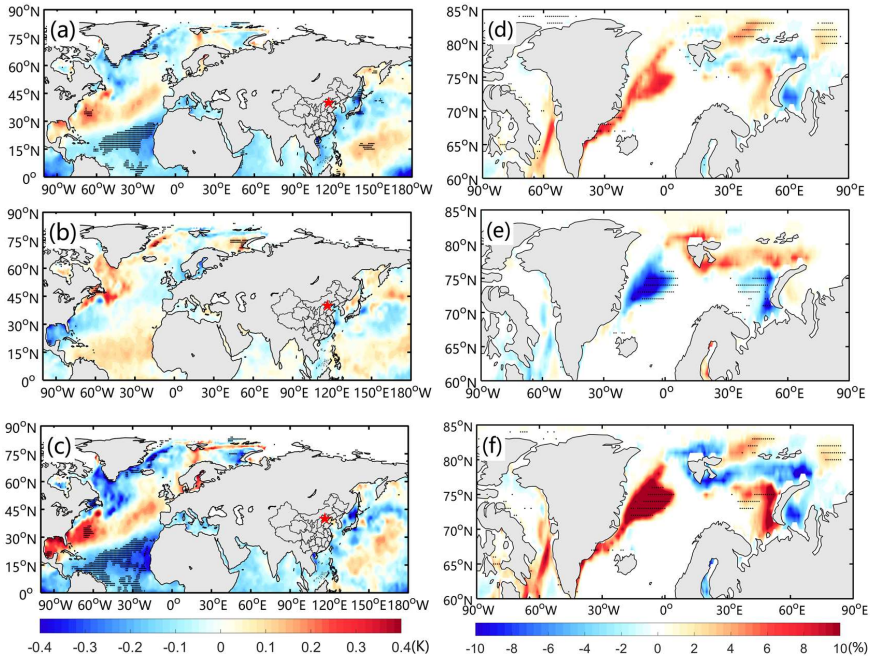

764

765 **Figure 6.** Composite SST anomalies and SIC anomalies for **(a, d)** winters (1988, 1996, 1998, 2005,

766 2007, 2008, 2011–15) with the greatest number of persistent haze days and **(b, e)** winters (1980, 1982–

767 84, 1986, 1987, 1994, 1995, 1999, 2003, 2010) with the lowest number of persistent haze days, and **(c,**

768 **f)** their differences. The dotted areas show values that are above the 95% confidence level based on a

769 Monte-Carlo test with 10,000 simulations.

770

771

772

773

774

775

https://doi.org/10.5194/acp-2020-823
Preprint. Discussion started: 14 January 2021

Atmospheric Chemistry and Physics Discussions

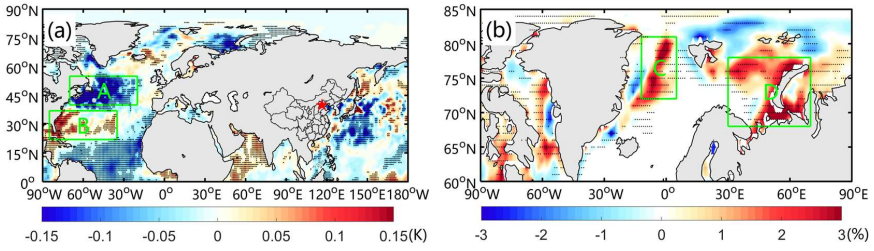

776

777 **Figure 7. (a)** Composite SST anomalies and **(b)** SIC anomalies for the 10 days before the first day of
778 the 65 persistent haze events. The dotted areas show values that are above the 95% confidence level
779 based on the two-sided Student's *t*-test. The green rectangles A and B in **(a)** denote a north region (40°
780 N–55° N, 70° W–20° W) and a south region (22° N–37° N, 85° W–35° W) over the North Atlantic,
781 and the green rectangles C and D in **(b)** denote the Greenland Sea (12° W–5° E, 72° N–81° N) and the
782 Barents–Kara Sea (30° E–70° E, 68° N–78° N), respectively

783

784

785

786

787

788

789

790

791

792

793

https://doi.org/10.5194/acp-2020-823
Preprint. Discussion started: 14 January 2021

Atmospheric Chemistry and Physics Discussions

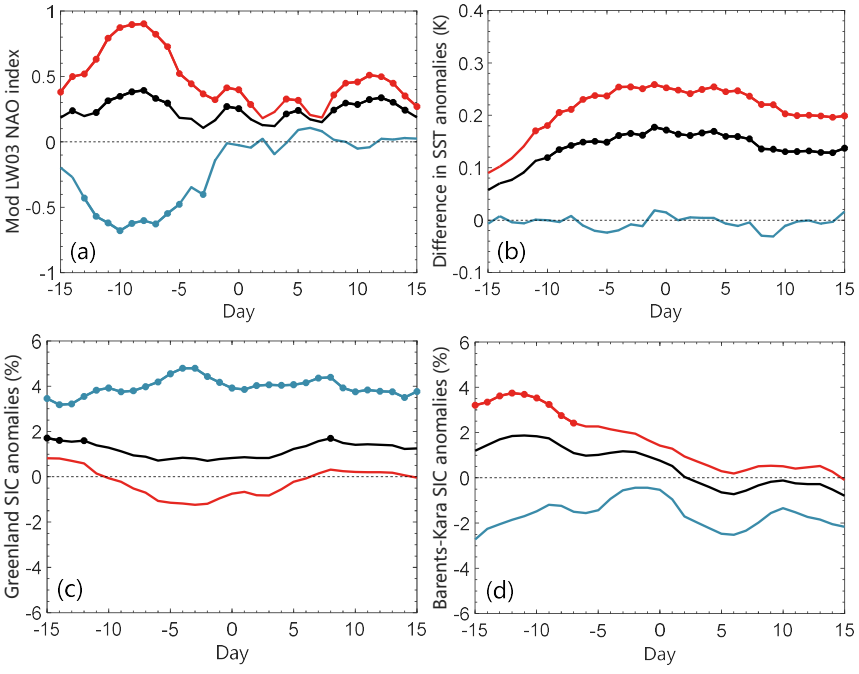

Figure 8. Composite daily time series of the **(a)** modified LW03 NAO index, **(b)** difference in the SST anomalies over the two regions, as presented in Figure 7a, **(c, d)** region-averaged SIC anomalies in the **(c)** Greenland Sea (marked by C in Figure 7b) and **(d)** Barents–Kara Sea (marked by D in Figure 7b) for the 65 persistent haze events (black), 43 NAO+-related persistent haze events (red) and 22 NAO−-related persistent haze events (blue) from Day −15 to Day 10. The difference in the SST anomalies is calculated by subtracting the region-averaged SST anomalies in the north (rectangle A) from the region-averaged SST anomalies in the south (rectangle B) (i.e., B minus A). The persistent haze event that is related to NAO+ (NAO-) is selected when its averaged NAO index is positive (negative) from Day -10 to Day -6 of the persistent haze event.

https://doi.org/10.5194/acp-2020-823
Preprint. Discussion started: 14 January 2021

Atmospheric Chemistry and Physics Discussions

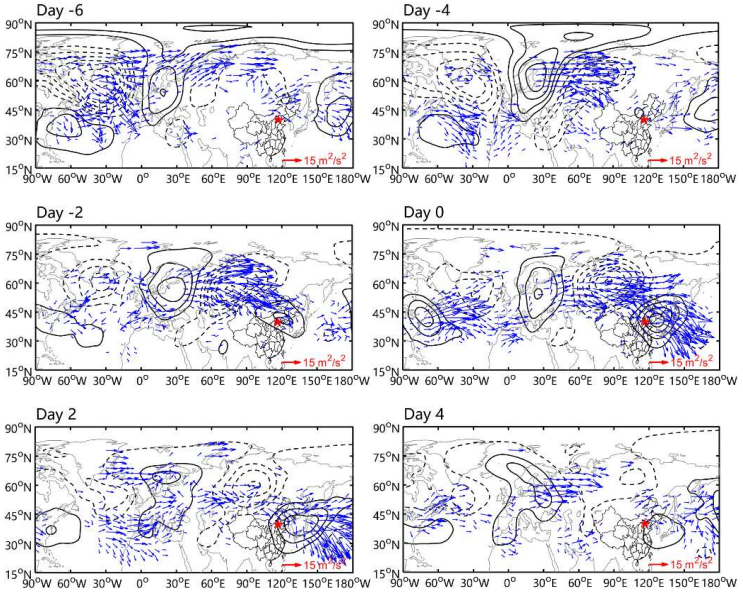

(a)

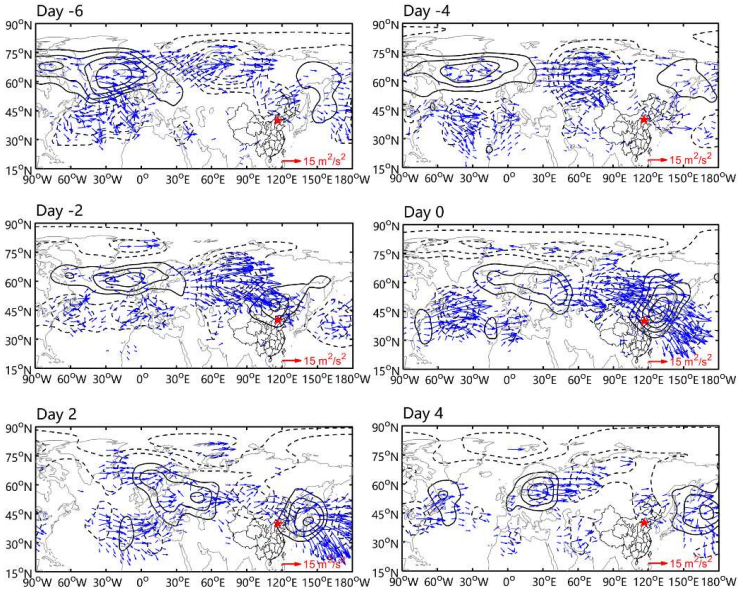

(b)

Figure 9. Instantaneous fields of composite daily Z500 anomalies (contours, interval = 20; units: gpm), SAT anomalies (shading; units: K) and horizontal components of W (vectors; units: m^2/s^2) for

https://doi.org/10.5194/acp-2020-823
Preprint. Discussion started: 14 January 2021

Atmospheric Chemistry and Physics Discussions

persistent haze events **(a)** related to NAO+ (43 events) and **(b)** related to NAO− (22 events) from Lag −6 to Lag 4. Only W vectors above 2 m^2/s^2 are plotted.

https://doi.org/10.5194/acp-2020-823
Preprint. Discussion started: 14 January 2021

Atmospheric Chemistry and Physics Discussions

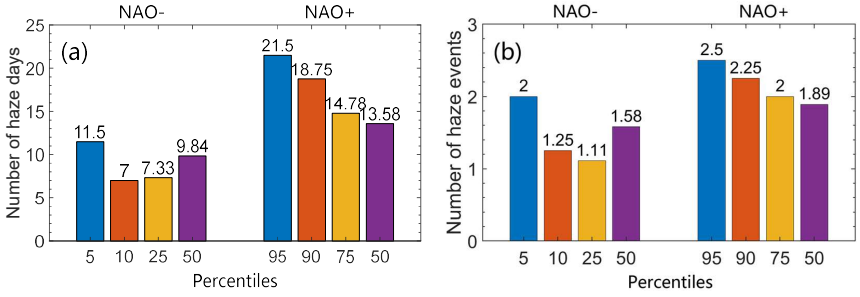

824

825 **Figure 10.** Averaged number of winter **(a)** haze days and **(b)** haze events during NAO+ winters and

826 NAO− winters. The blue, orange, yellow and violet bars on the left and right denote winters with an

827 NAO index larger than the 5th, 10th, 25th and 50th percentiles (NAO− winters) and winters with the

828 NAO index smaller than the 95th, 90th, 75th and 50th percentiles (NAO+ winters), respectively.

829